CHAPTER VI
AN EXPERIMENTAL STUDY ON THE EFFECTS OF TEMPERATURE ON MIXED THF-CH_4 HYDRATES FORMATION AND DISSOCIATION RATES

6.1 Abstract

This work investigated the effect of experimental temperature on methane hydrate formation and dissociation rates in 5.56 mol% THF solution. The experiments were conducted at 8 MPa and different temperatures including 4, 7, 10, and 15 °C in the quiescent condition. The results indicated that the methane hydrate formation rates at 4 °C is enhanced in all temperatures compared to the pure water system. Although the fastest induction time is observed in the experiment conducted at 4 °C, the experiment conducted at 15 °C shows the highest water conversion to hydrate in the range of 83.5 – 85.0 %. In addition, the experiment conducted at 10 °C reaches 90 % of the final methane uptake (t_{90}) faster than other temperatures. The stability of methane hydrate formation at high temperature is lower than at low temperature. Furthermore, the methane gas can be recovered at about 75.1 – 91.4 % from its hydrate by increasing the temperature to 34 °C.

Keywords: Methane; Mixed hydrates; Tetrahydrofuran; Formation; Dissociation; Kinetics; Promoter

6.2 Introduction

Natural gas hydrates are naturally formed in the marine sediment and permafrost regions. Natural gas hydrates, primary composed of methane, are non-stoichiometric crystalline substances formed by water and light natural gases. In the hydrate crystals, gas molecules are entrapped in the water cages formed by hydrogen bonds. The cages are composed of cavities of various sizes occupied by the gas molecules and stabilized by van der Walls forces between water molecules and the encapsulated gas molecules (Englezos, 1993; Sloan and Koh, 2008). The hydrogen-bonded water molecules can form the polyhedron hydrate cages of varying sizes from the smallest dodecahedron (5^{12}) to the largest isocahedron ($5^{12}6^8$) (Wu *et al.*,

2014; Sloan and Koh, 2008). The stacking of polyhedron consisted of three well-known crystalline structures of the hydrates including sI (two 5^{12} and six $5^{12}6^2$), sII (sixteen 5^{12} and eight $5^{12}6^4$), and sH (three 5^{12}, two $4^35^66^3$, and one $5^{12}6^8$) (Udachin *et al.*, 2002; Sloan and Koh, 2008).

Under favorable conditions, the mixture of water and small gas guest molecules such as methane or carbon dioxide usually form sI hydrates. The medium size of guest molecules such as tetrahydrofuran (THF) or isobutane may form sII hydrates. The sH hydrate could be formed by the presence of both small and large sizes of gas guest molecules, such as methylcyclohexane and methane (Ripmeester *et al.*, 1987; Udachin *et al.*, 2002). The amount of natural gas trapped in the natural gas hydrate formation is so abundant, and it is considered as a potential source of energy (Kvenvolden, 1993; Haq, 1999; Englezos and Lee, 2005). Because of the high capacity per unit volume of the hydrate (170 m^3 of methane gas at STP can be stored in a unit volume of the hydrate) (Koh *et al.*, 2011; Englezos and Lee, 2005; Kang and Lee, 2000; Linga *et al.*, 2007; Sloan, 2003; Veluswamy *et al.*, 2014b), the gas hydrate-based technology are also considered as a good medium for the storage and transportation of large quantities of gas such as hydrogen, natural gas, and carbon dioxide (Chapoy *et al.*, 2007; Kim *et al.*, 2009; Sugahara *et al.*, 2009; Ogata *et al.*, 2010; Gbaruko *et al.*, 2007; Chatti *et al.*, 2005). However, the slow hydrate formation rate, low gas consumption, and its stability are still the crucial issues to apply the hydrate-based technology for storing and transportation of gas.

It has been reported that THF is a very effective thermodynamic promoter of methane hydrates, which shifts the hydrate phase equilibrium and extends the stability zone of the hydrate (Susilo *et al.*, 2008; Chari *et al.*, 2012; Strobel *et al.*, 2009). Nevertheless, THF itself can form the sII hydrate with water without the other helping gas molecules. Due to the large-sized molecule, THF molecules always occupy the large cages ($5^{12}6^4$) of sII regardless of THF concentrations (Jones *et al.*, 2010; Delahaye *et al.*, 2006; Anderson *et al.*, 2007; Prasad *et al.*, 2009), and leave the small cages (5^{12}) vacant, which could be occupied by the small gas guest molecules such as methane, carbon dioxide, and hydrogen. Currently, many studies investigated the gas hydrate formation with the presence of THF. The hydrogen hydrate formation pressure was reduced by adding THF in the liquid phase (Florusse

et al., 2004), and a small amount of THF can help enhancing the occupancy of hydrogen hydrates resulting in increasing the amount of hydrogen capacity (Sugahara *et al.* 2009). Not only was the hydrogen uptake capacity increased with the presence of THF but also the rate of hydrogen hydrate growth; however, it was not stable compared to other promoters including butylammonium bromide and cyclopentane (Veluswamy and Linga, 2013; Veluswamy *et al.*, 2014a). Moreover, the presence of 6 mol% THF in liquid phase extended the methane phase equilibrium to a lower pressure and higher temperature by forming sII hydrates (Mohammadi and Richon, 2009; Chari *et al.*, 2012). The water conversion in mixed THF-CH_4 hydrates was lower than that in the simple CH_4 hydrate; in addition, the dissociation rate was lower with the increase in the storing pressure (Giavarini *et al.*, 2008). Later, it was observed that the overall hydrate yield in mixed THF-CH_4 hydrates was always more than pure CH_4 hydrate and the increase in the initial pressure decreased the induction time of mixed THF-CH_4 hydrates (Sharma *et al.*, 2014). Many studies investigated the thermodynamic and kinetic effects of mixed THF-CH_4 hydrates formation. To the best of our knowledge, there is less information on the effect of temperature on mixed THF-CH_4 hydrates formation and dissociation rates. This study provided the effect of temperature on methane hydrate formation and dissociation rates by using a theoretical concentration of THF at 5.56 mol%. Moreover, the induction time, methane consumption, water conversion to hydrate, and the time to reach 90 % of the final methane uptake (t_{90}) were reported.

6.3 Experimental

6.3.1 Materials and Apparatus

Ultra high purity methane (99.999 %, Labgaz Thailand Co., Ltd.), distilled deionized water, tetrahydrofuran (THF, 99.8 %, Lab-Scan, Thailand), were used for the methane hydrate formation and dissociation experiment. The THF concentration of 5.56 mol% was prepared. The methane hydrate formation and dissociation apparatus of Siangsai *et al.* (2015) was used. Briefly, the apparatus consists of a high-pressure stainless steel crystallizer (50 cm^3) and supply vessel immersed in a temperature-controlled bath. The pressure transmitter with 0.13 %

global error was used to measure the pressure. Four k-type thermocouples were located at different positions; at the top (T1), middle (T2), bottom (T3) of solution, and T4 at the bottom of the crystallizer. A data logger (AI210, Wisco Industrial Instruments, Thailand) was connected to a computer to record the data during the experiment. All experiments were carried out in the quiescent condition with a fixed amount gas and water in the closed system.

6.3.2 Hydrate Formation Experiment

Approximately, 30 cm^3 of 5.56 mol% THF solution was poured into the crystallizer. The crystallizer was pressurized to 0.5 MPa and depressurized to atmospheric pressure twice to eliminate the presence of air in the system. The experimental temperatures was set at 4, 7, 10, 15 °C and constant pressure at 8 MPa. The data was recorded every 10 s by the data logger. During the hydrate formation, the pressure in the crystallizer dropped due to the gas consumption. The experiments continued until there was no further pressure drop at least 1 h. The pressure and temperature data were used to calculate the moles of methane consumed by equation 6.1;

$$\Delta n_{H,\downarrow} = n_{H,0} - n_{H,t} = \left(\frac{PV}{zRT}\right)_{G,0} - \left(\frac{PV}{zRT}\right)_{G,t} \tag{6.1}$$

where $\Delta n_{H,\downarrow}$ is the number of moles of gas consumed for hydrate formation at the end of experiment. $n_{H,0}$ is the number of moles of hydrates at time zero. $n_{H,t}$ is the number of moles of the hydrates at time t. Subscripts of $G,0$ and G,t represent the gas phase at time zero and time t, respectively. P and T are the pressure and temperature in the system. V is the volume of gas phase in the crystallizer. R is the universal gas constant. z is the compressibility factor calculated by Pitzer's correlation (Veluswamy and Linga, 2013; Babu *et al.*, 2013).

The conversion of water to hydrates in the THF solution was calculated with equation 6.2 (Veluswamy and Linga, 2013);

$$\text{Conversion (\%)} = \frac{\left(\Delta n_{H,\downarrow} + \Delta n_{THF}\right) \times \text{Hydration number}}{n_{H_2O}} \times 100 \qquad (6.2)$$

where n_{H_2O} is the number of moles of water in the system. The hydration number of 5.66 was used to calculate the conversion in THF solution, based on structure II (sII) hydrate. Δn_{THF} is the number of moles of THF consumed for the hydrate formation at the end of experiment, as seen in equation 6.3 (Veluswamy and Linga, 2013);

$$\Delta n_{THF} = \Delta n_{H,\downarrow} \times \frac{\text{number of large cages}}{\text{number of small cages}} \qquad (6.3)$$

6.3.3 Hydrate Dissociation Experiment

After completion of methane hydrate formation, the hydrate was dissociated by thermal stimulation. The pressure in the crystallizer was reduced carefully to 6.5 MPa by releasing the free gas in the system. Then, the temperature was increased from the formation temperatures (4, 7, 10, and 15 °C) at the same heating rate for all experiments to 34 °C. This point was marked as time zero for the dissociation experiment. The hydrate dissociates when the temperature in the crystallizer crosses the equilibrium phase boundary, corresponding to the desired experimental pressure at 6.5 MPa. The moles of methane released from the hydrate at any time during the hydrate dissociation can be calculated by equations 6.1 by replacing $\Delta n_{H,\downarrow}$ with $\Delta n_{H,\uparrow}$, which represents the number of moles of gas released from the hydrate. The methane recovery is calculated by equation 6.4 as a function of time for any dissociation experiment based on its information of formation experiment (Haligva *et al.*, 2010; Linga *et al.*, 2009).

$$\text{\%methane recovery} = \frac{(\Delta n_{H,\uparrow})}{(\Delta n_{H,\downarrow})} \times 100 \qquad (6.4)$$

6.4 Results and Discussion

6.4.1 Hydrate Formation

Table 6.1 summarizes the THF-CH_4 hydrate formation at 8 MPa. The subcooling temperature (ΔT) represents the difference between the studied temperature and the equilibrium temperature at 8 MPa. The equilibrium temperature at 8 MPa of methane hydrate with the presence of 5.56 mol% THF is 30 °C (Lee *et al.*, 2012; Sharma *et al.*, 2014). The induction time in Table 6.1 indicates the first methane hydrate formation. All experiments in Table 6.1 show fast methane hydrate formation within 7 min compared to pure water, which does not show the evidence of methane hydrate formation until 48 h. Moreover, the temperature influences the rate of methane hydrate formation as expected. In other words, increasing the temperature leads to the increase in the induction time, as shown in Figure 6.1. Therefore, at lower temperature or higher subcooling temperature, the hydrate can be formed faster.

The methane hydrate growth rates can be represented by t_{90}, which is the time to achieve 90 % of the final methane uptake. The t_{90} of all experiments are listed in Table 6.1. Figure 6.2 shows the effect of temperature on the t_{90} with the presence of 5.56 mol% THF. The effect of temperatures on the t_{90} is different from that on the induction time. There is no significant difference of t_{90} from the experiments at 4 and 7 °C, which is higher than that at 10 °C. While the longest t_{90} of methane hydrate formation is observed in the experiment conducted at 15 °C. In other words, this result indicates that the experiment conducted at 10 °C shows the highest methane hydrate formation rate, based on t_{90}.

Figure 6.3 shows the methane uptake and temperature profiles of 5.56 mol% THF at 8 MPa and 4 °C. As seen from the figure, methane hydrate forms rapidly after introducing methane gas into the crystallizer, observed by the rapid methane consumption and the temperature spikes of heat released during the hydrate formation (exothermic process). It can be deduced that methane hydrate starts forming at the gas and liquid interface and moves down to the bottom of the crystallizer. After the first hydrate formation, methane gas is continually consumed to grow the hydrate crystal; thus, the hydrate formation at low temperature is very

dense and stiff, as seen in the inset. Therefore, the formation of methane hydrate may cover the interface of the liquid phase and block the gas to form the hydrate due to its high density, denoted as the deflection point in the figure, leading to the decrease in the gas diffusion and slow methane uptake until reaching the equilibrium at about 1.5 h.

However, the methane uptake and temperature profiles at higher temperature are different. Figure 6.4 presents the methane uptake and temperature profiles of the experiment conducted at 15 °C. From the figure, it is clearly seen that the hydrate formation starts at the interfacial of gas and liquid phase and moves downward to the bottom of the crystallizer, observed by the thermocouples at different positions in the crystallizer. Moreover, the porous hydrate is observed, as seen in the inset, which allows the methane gas diffuse through the porous hydrate formation and forms the hydrate crystals with free water, trapped between the porous hydrates. Hence, the subsequent methane hydrate formations can be observed due to porous hydrate. However, the time to reach the equilibrium of the experiment conducted at 15 °C is longer than the other temperatures.

Furthermore, to clarify the effect of temperature on the hydrate formation mechanism, comparison among the hydrate growth profiles during methane hydrate formation of the experiments conducted at different temperatures with the presence of 5.56 mol% THF at 8 MPa is shown in Figure 6.5. At the beginning (within 15 min), results from the experiments conducted at 4, 7, and 10 °C show almost the same hydrate growth rate, while, at 15 °C, the hydrate growth is slower than the others. As discussed previously, the hydrate layers are formed covering the interface of the aqueous phase as fast as the first methane hydrate is formed. In other words, the experiments conducted at 4 and 7 °C form the dense and stiff hydrate blocking the free gas to grow the hydrate crystals (Kang and Lee, 2010). This high density hydrate in experiments conducted at 4 and 7 °C are formed faster than that at 10 °C, as seen in the figure. That causes the slow kinetic rates after the hydrate is formed. In addition, at the equilibrium, the hydrate growth profiles are significantly different. In other words, the experiment conducted at 15 °C shows the highest methane uptake followed by the experiments conducted at 10, 4, and 7 °C, respectively. It can be noted that the hydrate growth of the experiments conducted at

4 and 7 °C reaches the equilibrium at about 1.5 h, followed by the experiment conducted at 10 and 15 °C about 2 and 3 h, respectively. This result indicates that higher temperature decreases the formation rates and extends the t_{90}. However, the experiment conducted at 10 °C shows the fastest t_{90} or the equilibrium condition, as seen in Figure 6.2. Moreover, it can be deduced that the different experiment temperatures cause the different in the hydrate growth rates, and the formation of dense and stiff hydrate is important factor, affecting the rates of hydrate growth.

Although the experiment conducted at 10 °C shows faster t_{90} than that at 15 °C, the methane consumption and the water conversion to hydrate are lower than that at 15 °C. The methane consumed and water conversion to hydrate are shown in Table 6.1. It is well known that, at higher temperature, the solubility of gas in THF could decrease (Gibanel *et al.*, 1993; Guha and Panda, 2008), which is expected to decrease the water conversion to hydrate at high temperature. However, the presence of 5.56 mol% THF in aqueous phase may change the mechanism of methane hydrate formation at the high temperature. It should be noted that the water conversion to hydrate depends on the methane hydrate growth mechanism. In other words, methane hydrate forms faster in the experiments conducted at 4, 7, and 10 °C, leading to the decrease in the methane consumption and water conversion to hydrate due to the dense and stiff hydrate at the interface of liquid solution blocks the gas to grow the hydrate crystals. At the same time, the slow methane hydrate formation rate is observed in the experiment conducted at 15 °C; therefore, the water conversion to hydrate is higher than that at the others because of the lower extent of hydrate layers blockage, as shown in Figure 6.6. It is believed that, at higher temperature, the THF molecules in solution vibrates and tries to evacuate from the solution to the gas phase, which acts as a nucleation sites of the hydrate formation; however, the hydrate formation at higher temperature is observed as porous hydrate. These results are in agreement with the theoretical prediction of the occupancy behavior of methane molecules in the small cages (5^{12}) of sII hydrate (Yoon, 2012). He used the predictive Soave-Redilich-Kwong (PSRK) group contribution method to predict the occupancy of methane in small cages of sII. The result indicates that methane molecules occupied in the small 5^{12} cages of sII gradually increases with the increase in the pressure and temperature, implying that methane molecules are readily

encaged in the small cages of sII hydrate, which was stabilized by THF molecules. In parallel, Kang and Lee (2010) observed that the increase in the experiment temperature led to the increase in the mass transfer of gas in liquid phase. Therefore, the hydrate formation is limited due to the limitation of mass transfer at lower temperature. Moreover, the final water conversion to hydrate in the range of 83.5 – 85.0 mol% is achieved at 15 °C.

6.4.2 Hydrate Dissociation

After the hydrate formation completion, the pressure in the crystallizer was reduced to 6.5 MPa, and thermal stimulation method was employed to recover methane gas from the hydrate formation. Figure 6.7 shows the typical methane released and temperature profiles during methane hydrate dissociation with the presence of 5.56 mol% THF. As seen in the figure, the temperatures of cooling water (T_{water}) increases as same as the temperature in the crystallizer until the change in temperature profiles in the crystallizer at about 1 h, caused by the balance of heat transfers between external heater (water) and methane hydrate dissociation (endothermic process) in the crystallizer, indicating the first released methane at about 26 °C. This point is marked as the dissociation temperature (T_d). After the temperature crosses T_d, methane hydrates decompose back to gas and liquid phases, and the amount of methane released obviously increases until reaching the plateau. In addition, the four thermocouples, located at different positions in the crystallizer, indicate that all methane hydrate regions begin to dissociate at the same dissociation temperature. However, the temperature at T2 increases first followed by T4, T3, and T1, meaning that the hydrate in each region could take different times to finish the dissociation due to the density of hydrate in each location. Moreover, the dissociation completes when the temperatures of all thermocouples reach the set point at 34 °C. From the dissociation experimental results, it can be deduced that the hydrate in different locations start to dissociate at the same temperature (T_d), but complete at different times. This behavior is observed in all dissociation experiments.

Table 6.2 shows the methane hydrate dissociation experimental conditions at 5 and 6.5 MPa with different temperature driving forces. The experimental number in the table corresponds to the methane hydrate formation

experimental conditions in Table 6.1. As seen form Table 6.2, with different temperature driving forces and the same initial pressure, the dissociation temperature is not significantly different, 25.8 – 26.6 °C at 6.5 MPa, while decreasing the initial pressure to 5 MPa, the dissociation temperature is about 24.1 – 25.0 °C. This result implies that the temperature driving force has little effect on the dissociation temperature but the initial pressure has a strong influence on the dissociation temperature, which corresponds to the hydrate phase equilibrium with the presence of 5.56 mol% THF. Moreover, the rates of methane released are also shown in Table 6.2. From the table, it can be seen that the rate of methane released at the 19 °C driving force is significantly higher than that of 30 °C. However, there is very little different from the driving force temperatures of 27 and 24 °C, as seen in the table. It can be deduced that the stability of methane hydrate formed at high temperature (low temperature driving force) is lower than at low temperature (high temperature driving force); therefore, the hydrate decomposes easier. Consequently, the hydrate formation at high temperature not only dissociates faster than that at low temperature but also recovers a higher amount of methane gas from the hydrate, as shown in Figure 6.8. In addition, the final methane recovery is in the range of 75.1 – 93.8 % for all methane hydrate dissociation experiments.

6.5 Conclusions

The effects of temperature on methane hydrate formation and dissociation kinetics were demonstrated by conducting the experiment with the presence of 5.56 mol% THF at 8 MPa and 4, 7, 10, and 15 °C in the quiescent condition. The results showed that, at the given temperatures, the methane hydrate formation rate was enhanced compared to pure water. The experiment conducted at 4 °C showed the fastest induction time due to the highest subcooling temperature; however, the highest water conversion to hydrate in the range of 83.5 – 85.0 % was observed in the experiment conducted at 15 °C due to lower extent of hydrate layers blockage. In addition, the experiment conducted at 10 °C reached t_{90} faster than other temperatures. The stability of methane hydrate at higher temperature was lower than that at lower temperature, leading to the ease in the decomposition. Furthermore, the

final methane recovery in the range of 75.1 – 93.8 % was obtained by increasing the temperature to 34 °C.

6.6 Acknowledgements

This work was supported by The Royal Golden Jubilee Ph.D. Program (2.P.CU/51/J.1), Thailand Research Fund; The Petroleum and Petrochemical College (PPC), Chulalongkorn University, Thailand; National Metal and Materials Technology Center (MTEC) (MT-B-53-CER-09-269-G), Thailand; Center of Excellence on Petrochemical and Materials Technology (PETROMAT), Thailand; UOP, A Honeywell Company, USA.

6.7 References

Anderson, R., Chapoy, A., and Tohidi, B. (2007) Phase relations and binary clathrate hydrate formation in the system H_2-THF-H_2O. Langmuir, 23, 3440-3444.

Babu, P., Yee, D., Linga, P., Palmer, A., Khoo, B.C., Tan, T.S., and Rangsunvigit, P. (2013) Morphology of methane hydrate formation in porous media. Energy Fuels, 27, 3364-3372.

Chapoy, A., Anderson, R., and Tohidi, B. (2007) Low-pressure molecular hydrogen storage in semi-clathrate hydrates of quaternary ammonium compounds. Journal of the American Chemistry Society, 129, 746-747.

Chatti, I., Delahaye, A., Fournaison, L., and Petitet, J.P. (2005) Benefits and drawbacks of clathrate hydrates: a review of their areas of interest. Energy Conversion and Management, 46, 1333-1343.

Chari, V.D., Sharma, D.V.S.G.K., and Prasad, P.S.R. (2012) Methane hydrate phase stability with lower mole fractions of tetrahydrofuran (THF) and tert-butylamine (t-BuNH_2). Fluid Phase Equilibria, 315, 126-130.

Delahaye, A., Fournaison, L., Marinhas, S., Chatti, I., Petitet, J.P., Dalmazzone, D., and Furst, W. (2006) Effect of THF on equilibrium pressure and dissociation enthalpy of CO_2 hydrates applied to secondary refrigeration. Industrial & Engineering Chemistry Research, 45, 391-397.

Englezos, P. (1993) Clathrate hydrates. Industrial & Engineering Chemistry Research, 32, 1251-1274.

Englezos, P. and Lee, J.D. (2005) Gas hydrates—A cleaner source of energy and opportunity for innovative technologies. Korean Journal of Chemical Engineering, 22(5), 671-681.

Florusse, L.J., Peters, C.J., Schoonman, J., Hester, K.C., Koh, C.A., Dec, S.F., Marsh, K.N., and Sloan, M.E. (2004) Stable low-pressure hydrogen clusters stored in a binary clathrate hydrate. Science, 30, 469-471.

Gbaruko, B.C., Igwe, J.C., Gbaruko, P.N., and Nwokeoma, R.C. (2007) Gas hydrates and clathrates: flow assurance, environmental and economic perspectives and the nigerian liquified natural gas project. Journal of Petroleum Science and Engineering, 56, 192-198.

Giavarini, C., Maccioni, F., and Broggi, A. (2008, July 6-10) Formation dissociation of CO_2 and CO_2-THF hydrates compared to CH_4 and CH_4-THF hydrates. Paper presented at The 6th International Conference on Gas Hydrates (ICGH 2008), Vancouver, Canada.

Gibanel, F., López, M.C., Royo, F.M., Santafé, J., and Urieta, J.S. (1993) Solubility of nonpolar gases in tetrahydrofuran at 0 to 30 C and 101.33 kPa partial pressure of gas. Journal of Solution Chemistry, 22, 211-217.

Guha, A. and Panda D. (2008) Solubility of some non-polar gases in mixed solvents. International Journal of Chemical Sciences. 6, 1147-1167.

Haligva, C., Linga, P., Ripmeester, J.A., and Englezos, P. (2010) Recovery of methane from a variable-volume bed of silica sand/hydrate by depressurization. Energy & Fuels, 24, 2947-2955.

Haq, B.U. (1999) Natural gas deposits-methane in the deep blue sea. Science, 285, 543-544.

Jones, C.Y., Zhang, J.S., and Lee, J.W. (2010) Isotope effect on eutectic and hydrate melting temperatures in the water-THF system. Journal of Thermodynamics, 2010, 1-6.

Kang, S.P. and Lee, H. (2000) Recovery of CO_2 from flue gas using gas hydrate: Thermodynamic verification through phase equilibrium measurments. Environmental Science & Technology, 34, 4397-4400.

ต้นฉบับ หน้าขาดหาย

Siangsai, A., Rangsunvigit, P., Kitiyanan, B., Kulprathipanja, S., and Linga, P. (2015) Investigation on the roles of activated carbon particle sizes on methane hydrate formation and dissociation. Chemical Engineering Science, 126, 383-389.

Sloan, E.D. (2003) Fundamental principles and applications of natural gas hydrates. Nature, 426, 353-359.

Sloan, E.D. and Koh, C.A. (2008) Clathrate hydrates of natural gases. 3rd ed. (pp 45-72). New York: CRC Press.

Strobel, T.A., Koh, C.A., and Sloan, E.D. (2009) Thermodynamic predictions of various tetrahydrofuran and hHydrogen clathrate hHydrates. Fluid Phase Equilibria, 280, 61-67.

Sugahara, T., Haag, J.C., Prasad, P.S.R., Warntjes, A.A., Sloan, E.D., Sum, A.K., and Koh, C.A. (2009) Increasing hydrogen storage capacity using tetrahydrofuran. Journal of the American Chemistry Society, 131, 14616-14617.

Susilo, R., Alavi, S., Ripmeester, J.A., and Englezos, P. (2008) Tuning methane content in gas hydrates via thermodynamic modeling and molecular dynamics simulation. Fluid Phase Equilibria, 263, 6-17.

Udachin, K.A., Ratcliffe, C.I., and Ripmeester, J.A. (2002) Single crystal diffraction studies of structure I, II and H Hydrates: structure, cage occupancy and composition. Journal of Supramolecular Chemistry, 2, 405-408.

Veluswamy, H.P., Chin, W.I., and Linga, P. (2014a) Clathrate hydrates for hydrogen storage: the impact of tetrahydrofuran, tetra-n-butylammonium bromide and cyclopentane as promoters on the macroscopic kinetics. International Journal of Hydrogen Energy, 39, 16234-16243.

Veluswamy, H.P., Kumar, R., and Linga, P. (2014b) Hydrogen storage in clathrate hydrates: Current state of the art and future directions. Applied Energy, 122, 112-132.

Veluswamy, H.P. and Linga, P. (2013) Macroscopic kinetics of hydrate formation of mixed hydrates of hydrogen/tetrahydrofuran for hydrogen storage. International Journal of Hydrogen Energy, 38, 4587-4596.

Wu, J.Y., Chen, L.J., Chen, Y.P., and Lin, S.T. (2014) Molecular dynamics study on

the equilibrium and kinetic properties of tetrahydrofuran clathrate hydrates . Journal of Physical Chemistry C, 119, 1400-1409.

Yoon, J.H. (2012) A theoretical prediction of cage occupancy and heat of dissociation of THF-CH_4 hydrate. Korean Journal of Chemical Engineering, 29, 1670-1673.

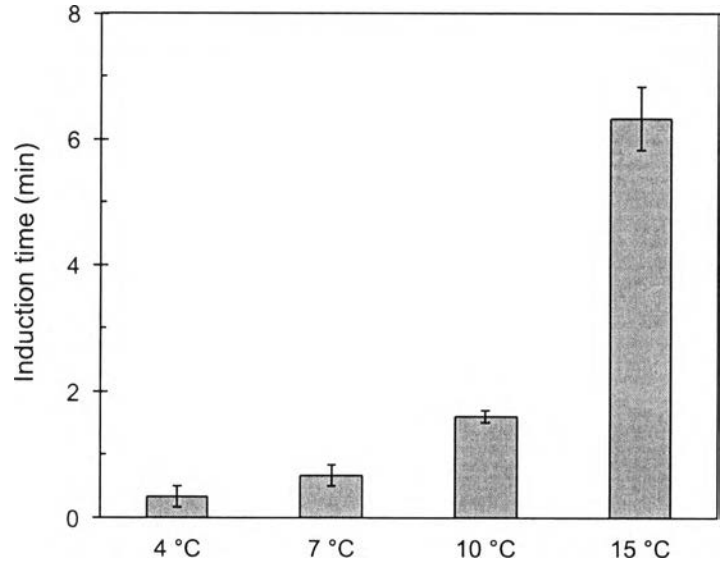

Figure 6.1 Effect of temperature on the induction time with the presence of 5.56 mol% THF.

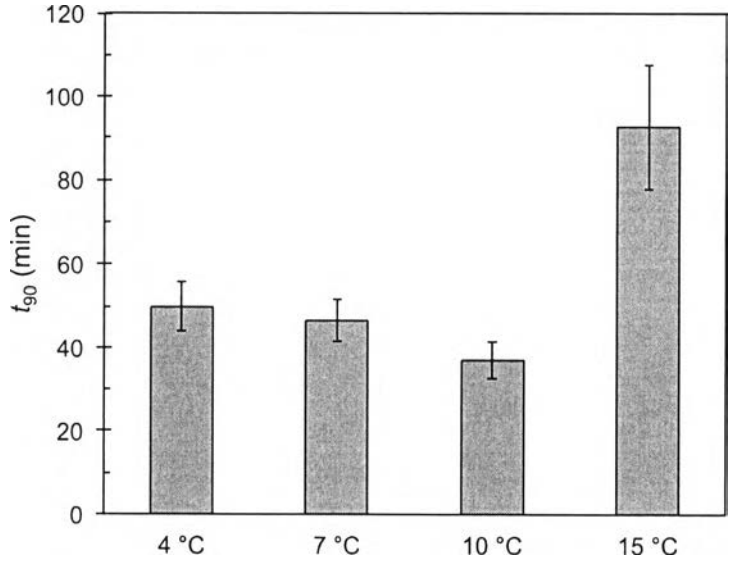

Figure 6.2 Effect of temperature on the t_{90} with the presence of 5.56 mol% THF.

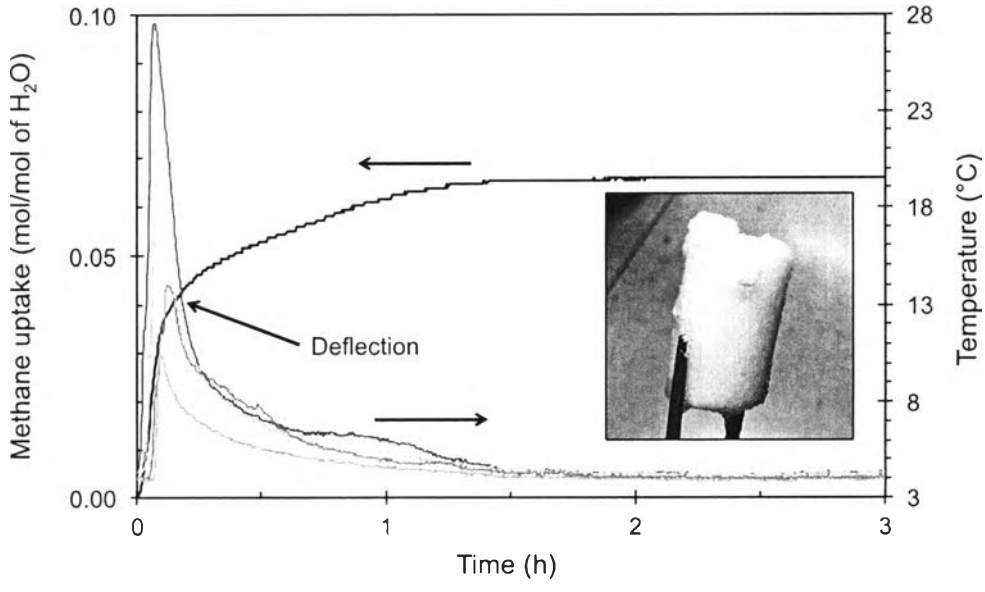

Figure 6.3 Methane uptake and temperature profiles during methane hydrate formation with the presence of 5.56 mol% THF at 8 MPa and 4 °C (Experiment 1, Table 6.1).

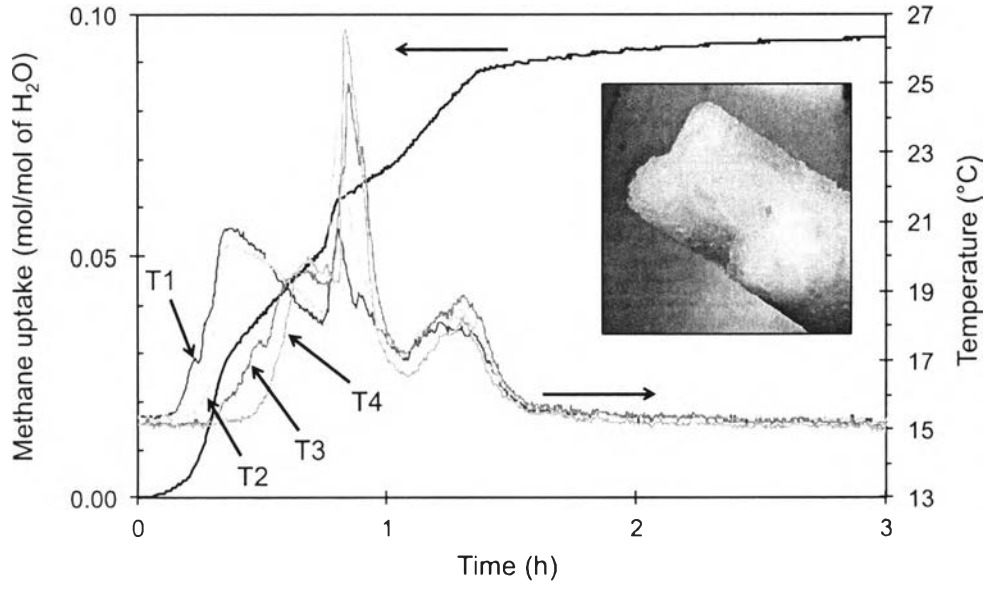

Figure 6.4 Methane uptake and temperature profiles during methane hydrate formation with the presence of 5.56 mol% THF at 8 MPa and 15 °C (Experiment 10, Table 6.1).

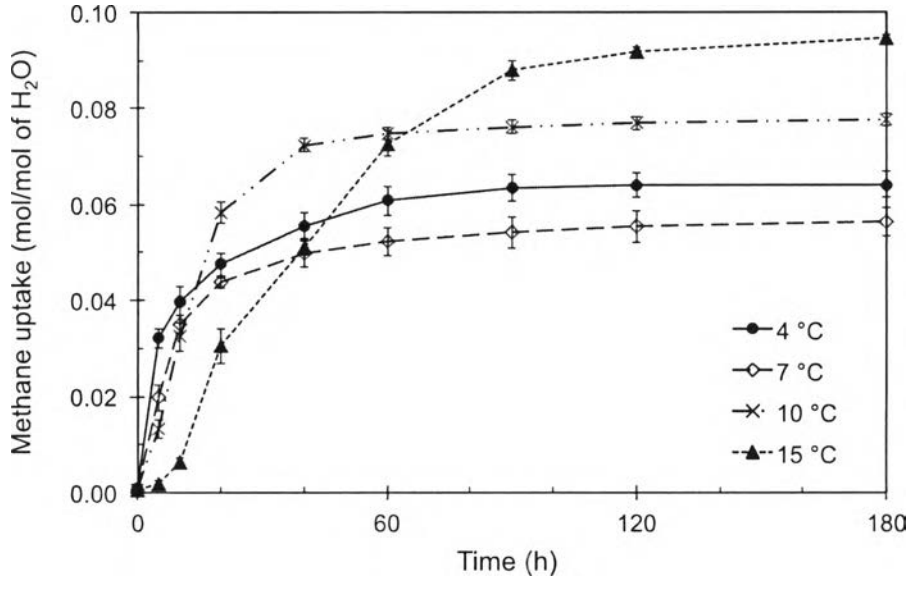

Figure 6.5 Hydrate growth profiles during methane hydrate formation of the experiments conducted at different temperatures with the presence of 5.56 mol% THF at 8 MPa (Time zero in the figure corresponds to the first point of hydrate growth).

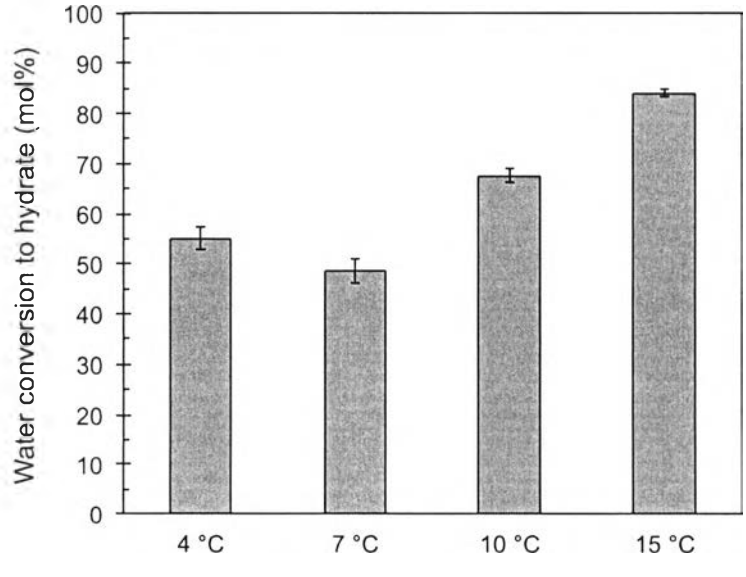

Figure 6.6 Effect of temperature on the water conversion to hydrates with the presence of 5.56 mol% THF.

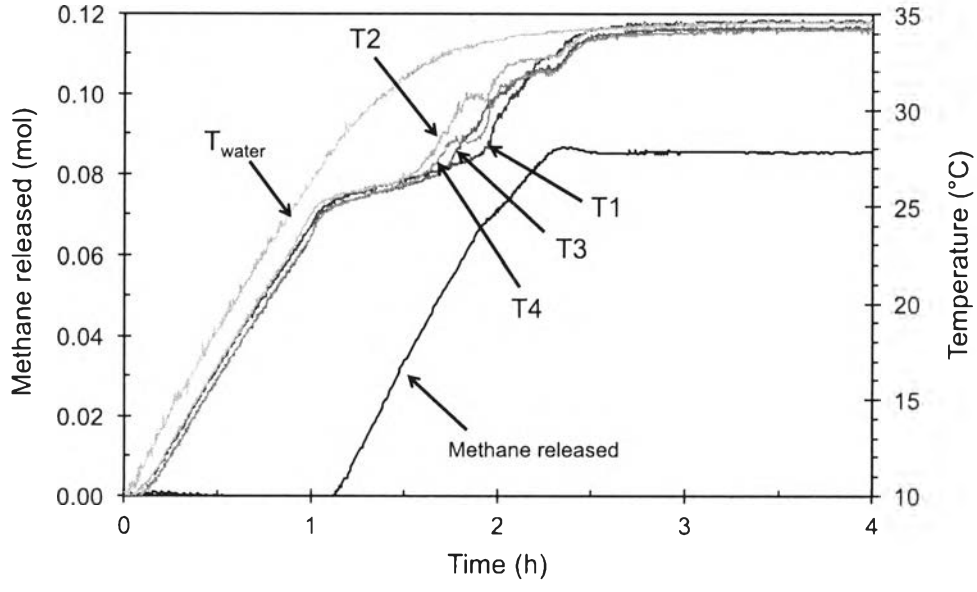

Figure 6.7 Methane released and temperature profiles during methane hydrate dissociation with the presence of 5.56 mol% THF (Experiment 7, Table 6.2).

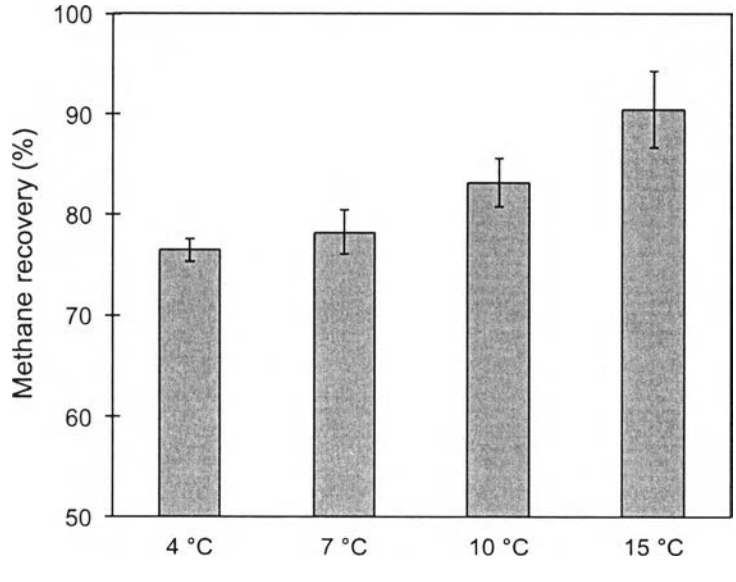

Figure 6.8 Effect of temperature on the methane recovery with the presence of 5.56 mol% THF.

Table 6.1 THF-CH_4 hydrate formation at 8 MPa

Exp. No.	Temperature (°C)	Subcooling Temperature(°C)	Induction Time* (min)	End of Experiment		
				t_{90}** (min)	Methane Consumed (mol/mol of H_2O)	Water Conversion to Hydrate (mol%)
			Water/CH_4			
0	4	26	DNF	-	-	-
			5.56 mol% THF/CH_4			
1	4	26	0.50	51.5	0.0668	56.7
2	4	26	0.17	54.7	0.0617	52.4
3	4	26	0.33	43.2	0.0661	56.1
4	7	23	0.83	52.5	0.0545	46.2
5	7	23	0.50	43.3	0.0603	51.2
6	7	23	0.67	44.0	0.0566	48.0
7	10	20	1.67	40.5	0.0799	67.9
8	10	20	1.50	32.0	0.0777	66.0
9	10	20	1.67	38.3	0.0811	68.9
10	15	15	5.83	78.0	0.0983	83.5
11	15	15	6.83	92.5	0.0988	83.9
12	15	15	6.33	107.8	0.1012	85.0

*Induction time is the first time of methane hydrate formation.

**t_{90} is the time required to reach 90 % of the final methane consumption including induction time.

DNF = Did not form hydrate

Table 6.2 THF-CH_4 hydrate dissociation at 34 °C

Exp. No.	Initial Pressure (MPa)	Dissociation Temperature, T_d* (°C)	Driving Force Temperature** (°C)	Rate of Methane Released (mol/h)	Methane Recovery (mol%)
1	6.5	25.9	30	0.0736	77.0
2	6.5	26.1	30	0.0812	75.1
3	6.5	25.8	30	0.0785	77.2
4	5.0	24.7	27	0.0879	80.7
5	6.5	26.6	27	0.0682	77.6
6	6.5	26.2	27	0.0869	76.4
7	5.0	25.0	24	0.0872	85.5
8	6.5	26.1	24	0.0813	83.5
9	6.5	26.2	24	0.0839	80.6
10	6.5	26.3	19	0.0977	91.4
11	6.5	26.1	19	0.1155	86.3
12	5.0	24.1	19	0.0837	93.8

*T_d is the dissociation temperature at which methane releases for the initial pressure.

**Driving force temperature = Final temperature (34 °C) – Experimental temperature